

Supplementary Figure Legends

Supplementary Figure 1 DDR1 regulated CXCL5 mRNA level in both MDA-PATC 148 and BxPC-3 cells. **A** DDR1 expression were analyzed by western blotting in MDA-PATC 148 and BxPC-3 cells with shRNA knockdown DDR1 (upper panel) and in MDA-PATC 148^{KD#32} and BxPC-3^{KD#32} cells with re-express DDR1 (bottom panel). **B** Neutrophil-related chemokines mRNA level were analyzed by real-time PCR in MDA-PATC 148 and BxPC-3 cells with shRNA knockdown DDR1. Data are mean \pm SD. $n = 3$, 3 independent experiments; one-way ANOVA with Sidak post hoc testing, $*p < 0.05$, $**p < 0.01$, $***p < 0.001$. **C** CXCL5 mRNA level by using real-time PCR (left panel) and CXCL5 protein level by using ELISA (right panel) in BxPC-3 cells with knockdown or re-express DDR1 were treated with collagen I for 3 hours. Data are mean \pm SD. $n = 4$, 3 independent experiments; one-way ANOVA with Sidak post hoc testing, $*p < 0.05$, $**p < 0.01$, $***p < 0.001$.

Supplementary Figure 2 DDR1 knockdown reduced CD11b+Ly6G+ neutrophils infiltration and liver metastasis. **A** DDR1 expression were analyzed by western blotting in KP^{wm}C cells with DDR1 knockdown. **B-D** C57BL/6J mice were orthotopically injected with KP^{wm}C (control and 2 of DDR1-deficient clones) cells for 9 weeks. **B left:** CD11b+Ly6G+ neutrophils infiltrated into primary tumors were analyzed by FACS. **right:** the calculation of CD11b+Ly6G+ neutrophils infiltration were based on left panel. $n=5$ mice, data performed in triplicate, one-way ANOVA with Sidak post hoc testing, $*p < 0.05$, $**p < 0.01$, $***p < 0.001$. **C** H&E staining of pancreas and liver section. *Arrow*: region of tumor, Scale bar, 50 μ m. The numbers of liver-met, $n=5$, Fisher's exact test, $*p < 0.05$. **D** ELISA showed CXCL5 level in plasma harvest from mice. $n=5$ mice, data performed in triplicate, one-way ANOVA with Sidak post hoc testing, $*p < 0.05$, $**p < 0.01$, $***p < 0.001$.

Supplementary Figure 3 DDR1-positive pancreatic cancer cells mediated NET formation from neutrophils and enhanced cancer cell invasion through NADPH oxidase-independently pathway. **A-C** Human neutrophils were co-culture with DDR1-knockdown of MDA-PATC 148 or BxPC-3 by matrigel transwell chamber, with or without NADPH oxidase inhibitor, PDA4 inhibitor, NE inhibitor and Dase I treatment, for 18 hours. **A** Cit-histone H3 expression were analyzed by western blotting. **B** NET structures were analyzed by immunofluorescence staining using DAPI (*blue*), anti-NE (*red*) and anti-histone (*green*) mAbs. *Scale bar*, 50 μ m. **C** The NET quantification is displayed as NET histone area (μ m²) /per 40X filed, 6 fields per group. Data are mean \pm SD. $n = 5$, 3 independent experiments; one-way ANOVA with Sidak post hoc testing, $*p < 0.05$, $**p < 0.01$, $***p < 0.001$.

Supplementary Figure 4 CXCL5 mediated cancer cell invasion through NET. The invaded MDA-PATC 148KD#32 cells were analyzed by matrigel transwell chamber, co-

culture with human neutrophils, with or without recombinant CXCL5, NDAPH oxidase, PDA4, NE inhibitor and DNase I treatment for 18 hours, and the average number of cells was calculated based on the number of cells found in 6 fields per chamber. Data are mean \pm SD. $n = 4$, 3 independent experiments; one-way ANOVA with Sidak post hoc testing, $*p < 0.05$, $**p < 0.01$, $***p < 0.001$.

Supplementary Figure 5 PKC θ -SYK-NF κ B pathway involved in DDR1 induced CXCL5 production and enhanced cancer cell invasion. **A** Activated NF- κ B were analyzed by western blotting using nuclear fraction in MDA-PATC 148 (upper panel) and BxPC-3 cells (bottom panel) with DDR1 knockdown. **B** Top 10 of protein level downregulation by using NF κ B phospho antibody array in MDA-PATC 148 cells with DDR1 knockdown. **C** phospho-NF- κ B P65 were detected by western blotting in MDA-PATC 148 with I κ B super-repressor mutation, with or without TNF- α treatment for 10 mins. **D** CXCL5 protein level were analyzed by ELISA in MDA-PATC 148 with I κ B super-repressor mutation, with or without collagen I treatment for 3 hours. **E** CXCL5 protein level were analyzed by ELISA in MDA-PATC 148 (upper panel) and BxPC-3 (bottom panel) with collagen I treatment, with or without R406, PKC inhibitor and Sotrastaurin treatment. **D-E** Data are mean \pm SD. $n = 4$, 3 independent experiments; one-way ANOVA with Sidak post hoc testing, $*p < 0.05$, $**p < 0.01$, $***p < 0.001$.

Supplementary Figure 6 7rh treatment reduced collagen I-induced CXCL5 production and NET-mediated cell invasion. **A** CXCL5 protein level were analyzed by ELISA in BxPC-3 with collagen I treatment, with or without 7RH treatment. Data are mean \pm SD. $n = 3$, 3 independent experiments; one-way ANOVA with Sidak post hoc testing, $*p < 0.05$, $**p < 0.01$, $***p < 0.001$. **B** Human neutrophils were co-culture with MDA-PATC 148 or BxPC-3 by matrigel transwell chamber, with or without 7RH treatment for 18 hours. The number of invaded cells were analyzed by immunofluorescence staining using DAPI and calculated based on the number of cells found in 6 fields /per chamber. Data are mean \pm SD. $n = 6$, 3 independent experiments; one-way ANOVA with Sidak post hoc testing, $*p < 0.05$, $**p < 0.01$, $***p < 0.001$.

Supplementary Figure 7 Collagen I induced CXCL5 level through STAT3-independent pathway. CXCL5 level were analyzed by ELISA in MDA-PATC 148 and BxPC-3 cells with cucurbitacin I pretreatment for 30 mins, with or without collagen I treatment for 3 hours. Data are mean \pm SD. $n = 4$, 3 independent experiments; unpaired two-tailed t-test.

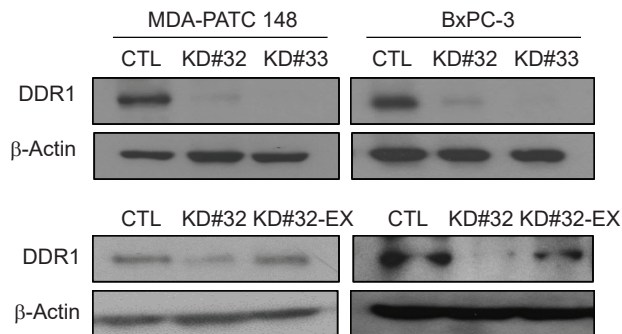
Supplementary Figure 8 Human neutrophils from human blood were checked by FACS using anti-CD16 and anti-CD66b antibodies.

Supplementary Figure 9 Quantification of IHC signal. Images were scanned using PE Vectra3 and processed by inform^R software, the H-Score were calculated by DBA signals/per selected cells. The score of each cells is 0 showed in blue, 1 showed in yellow, 2 showed in orange and 3 showed in brown.

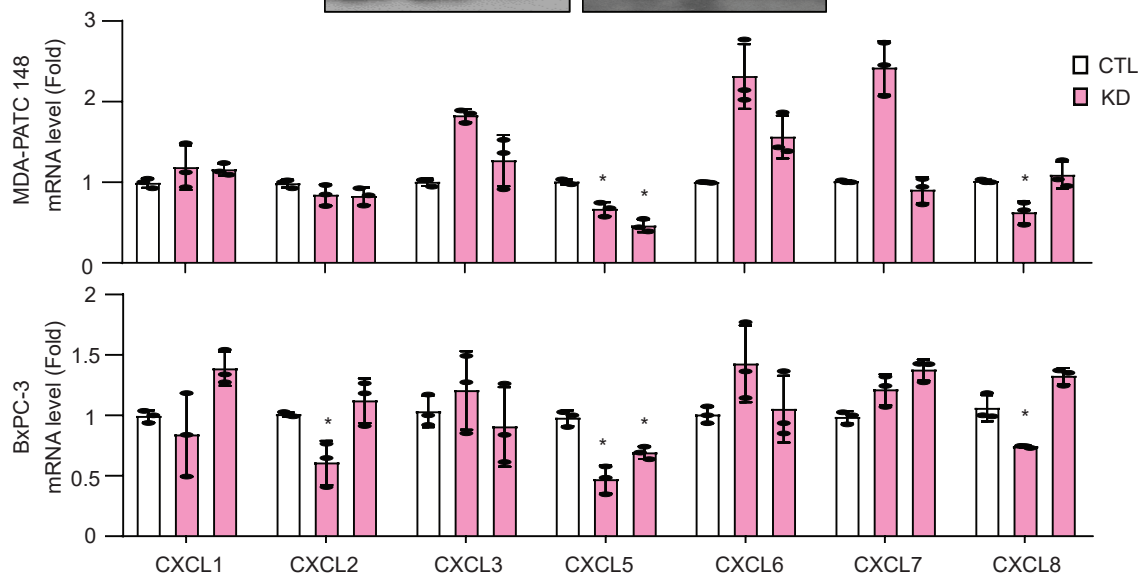
Supplementary Figure 10 Original luminescence images of the blots presented in the main text. Related to Figure 1-10.

Supplementary Table 1. The primers of real-time PCR and ChiP assay in the main text.

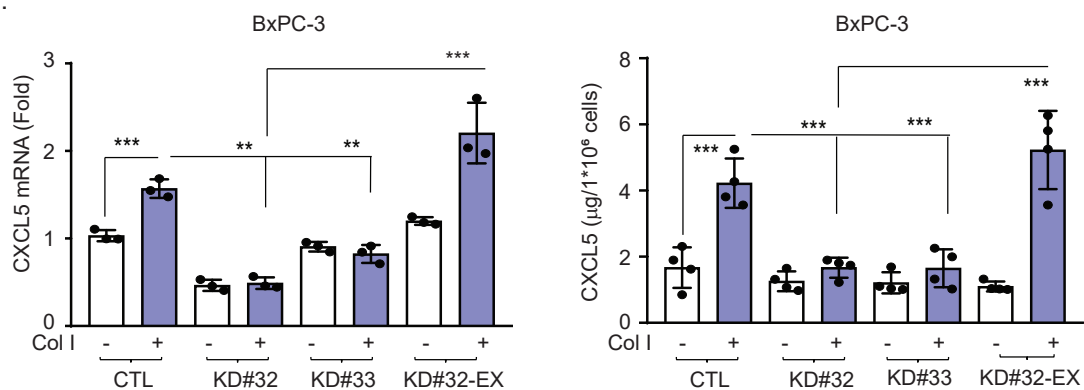
A.



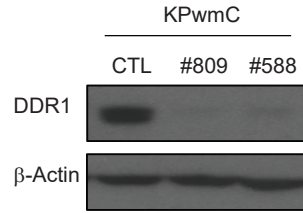
B.



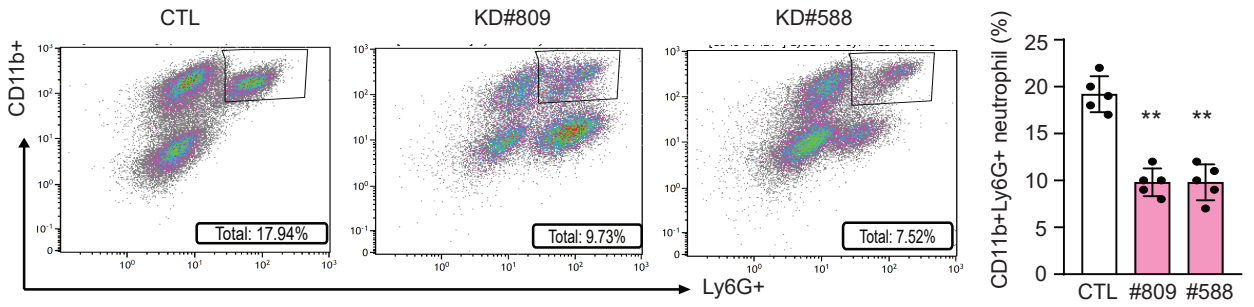
C.



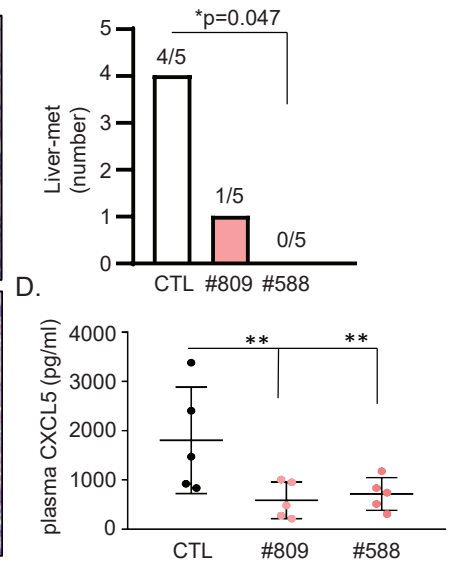
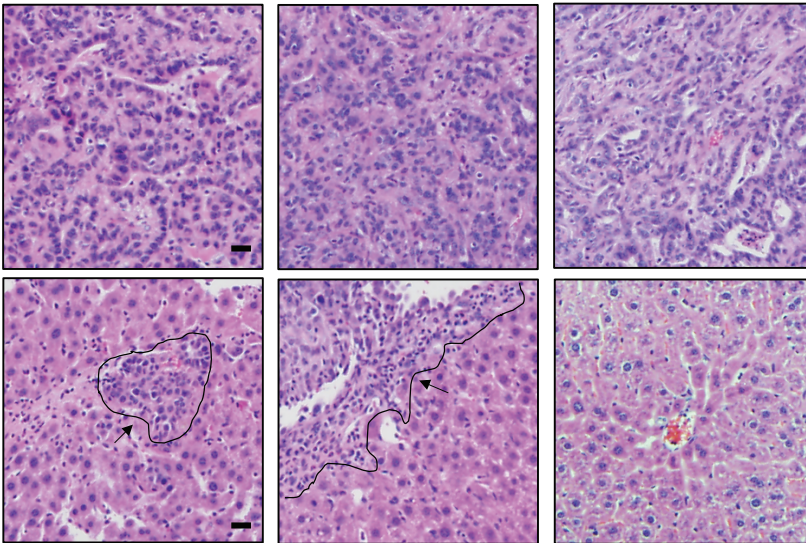
A.



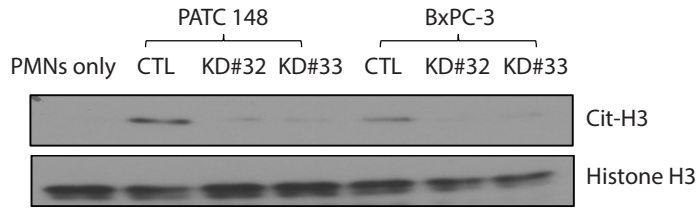
B.



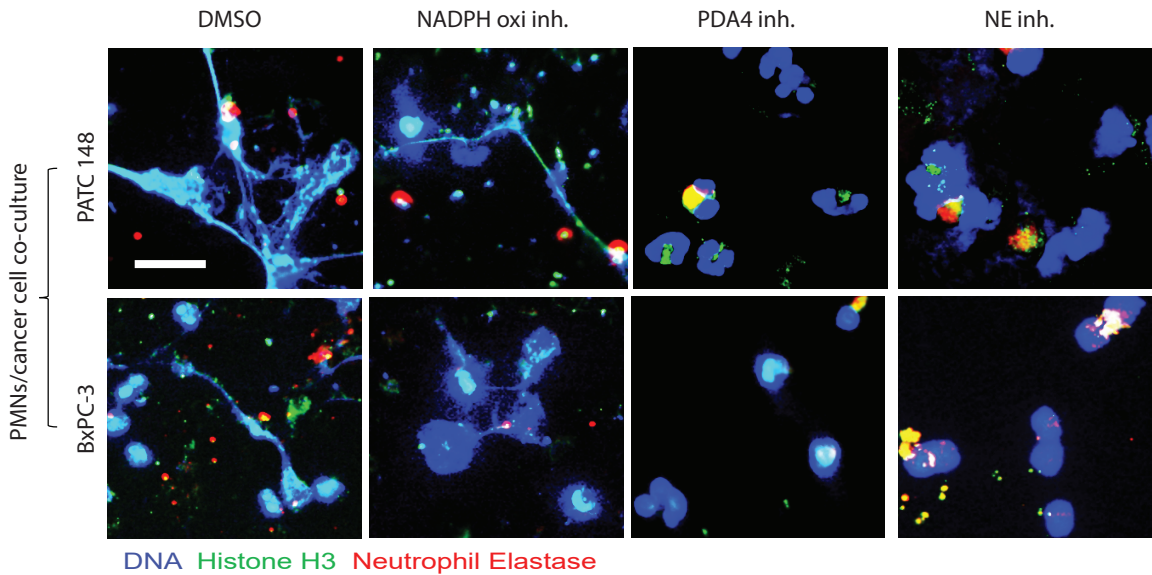
C.



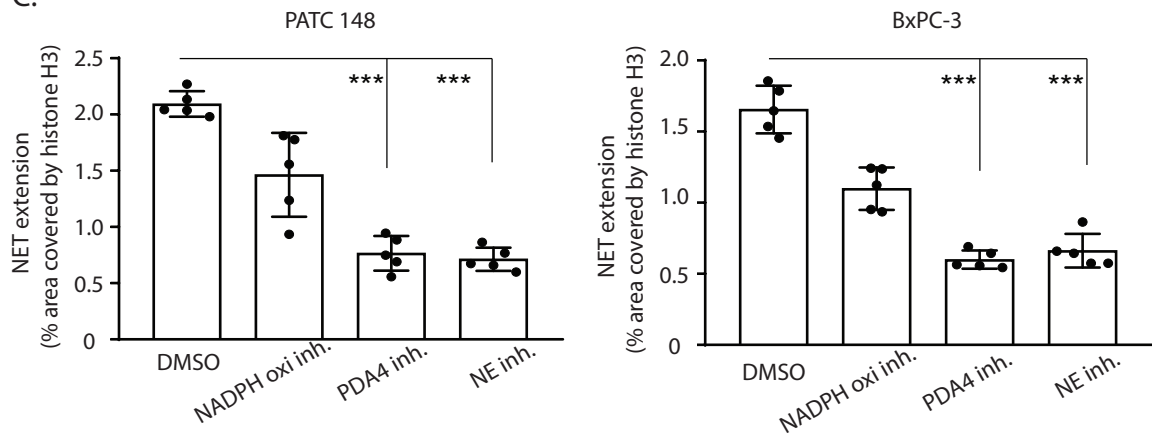
A.

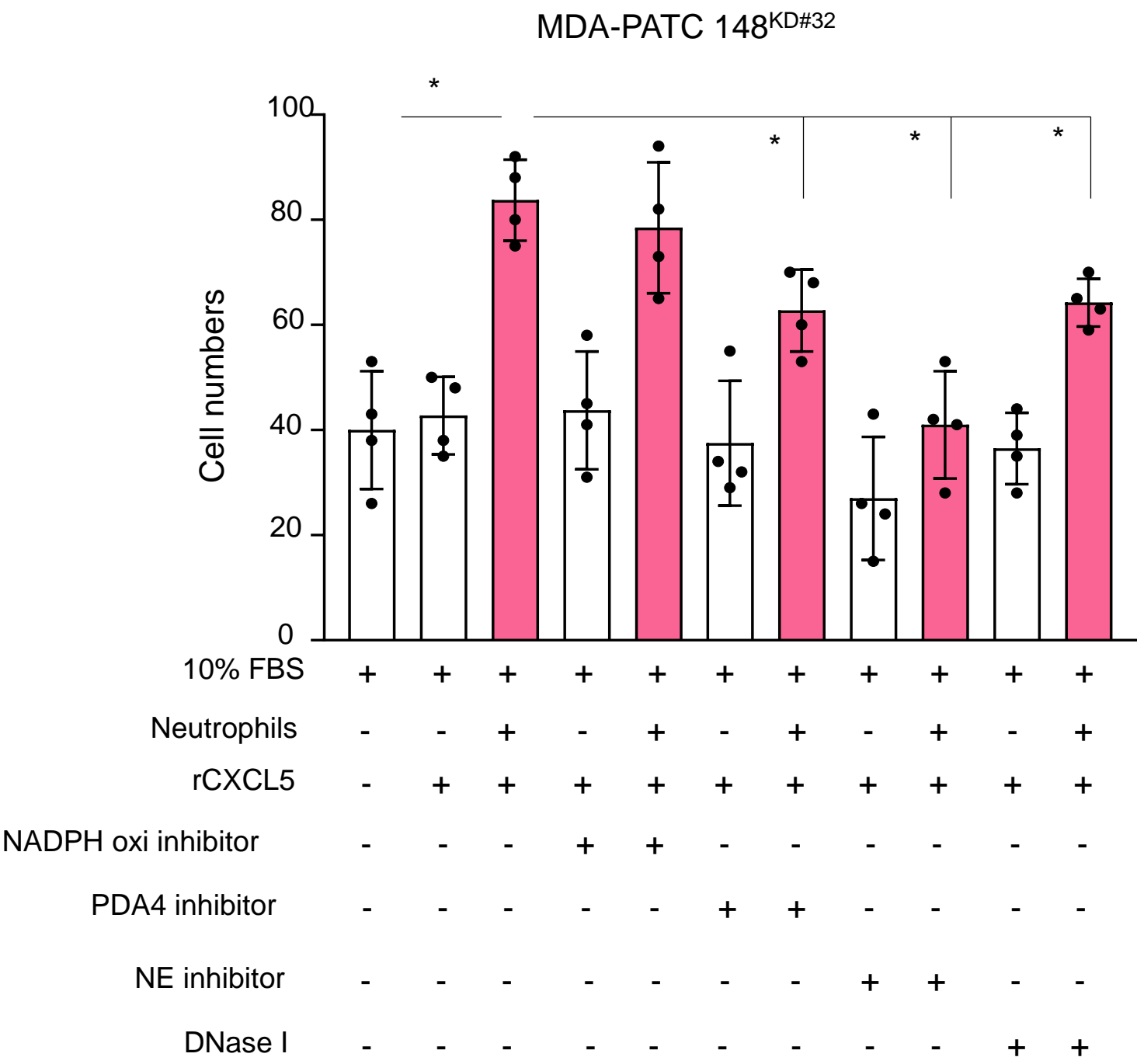


B.

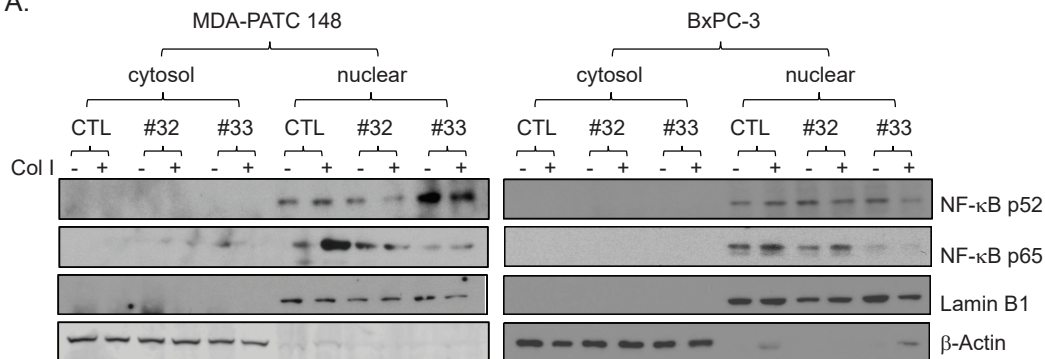


C.

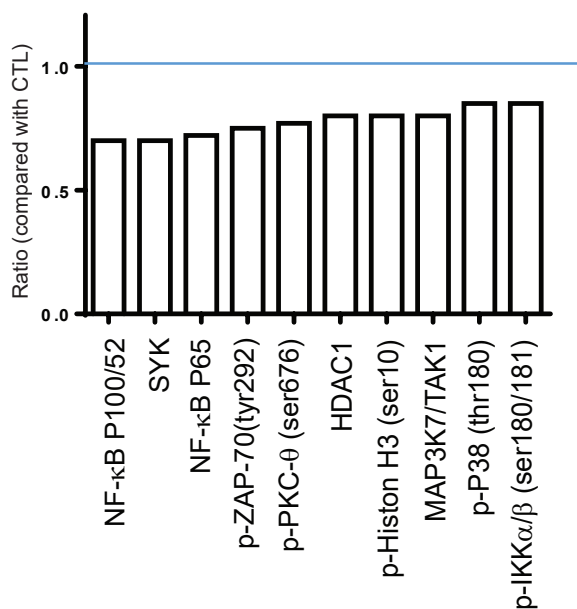




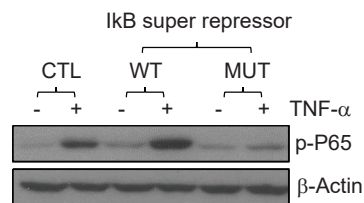
A.



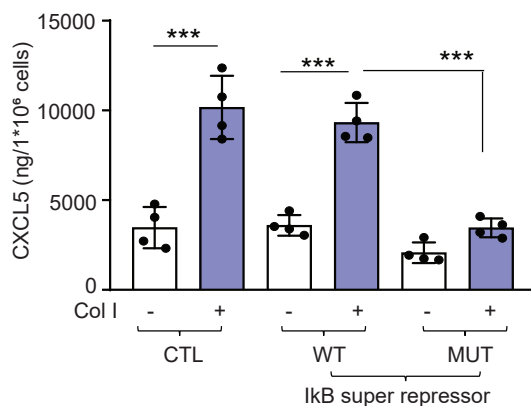
B.



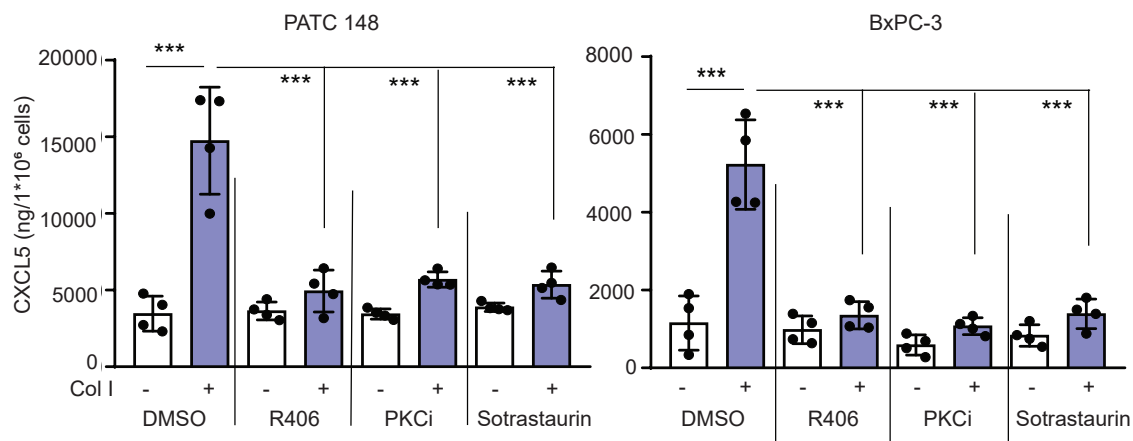
C.



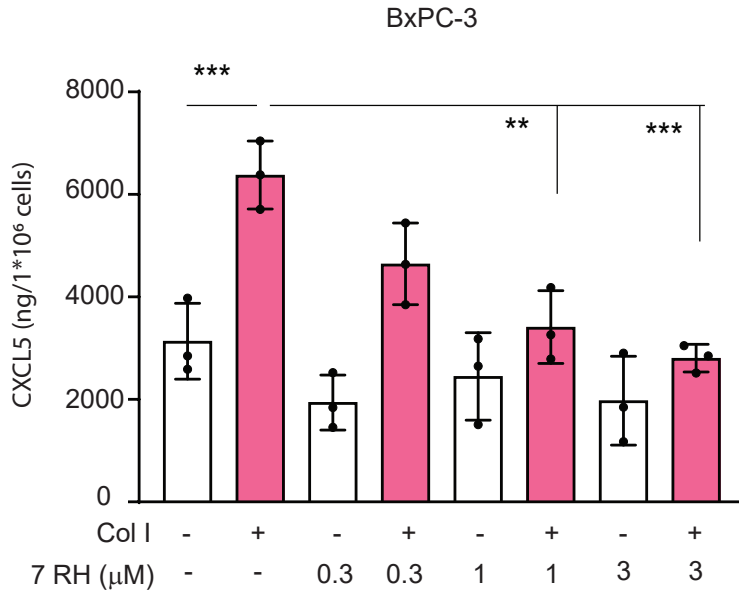
D.



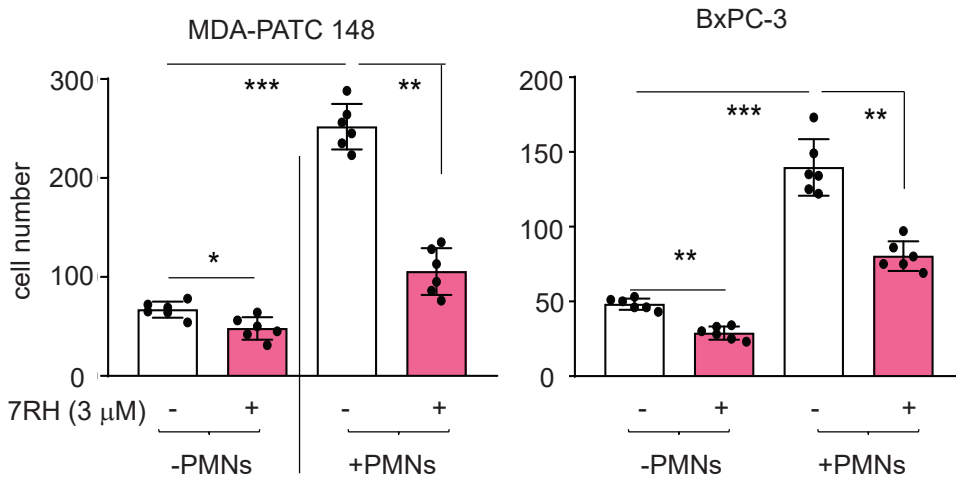
E.

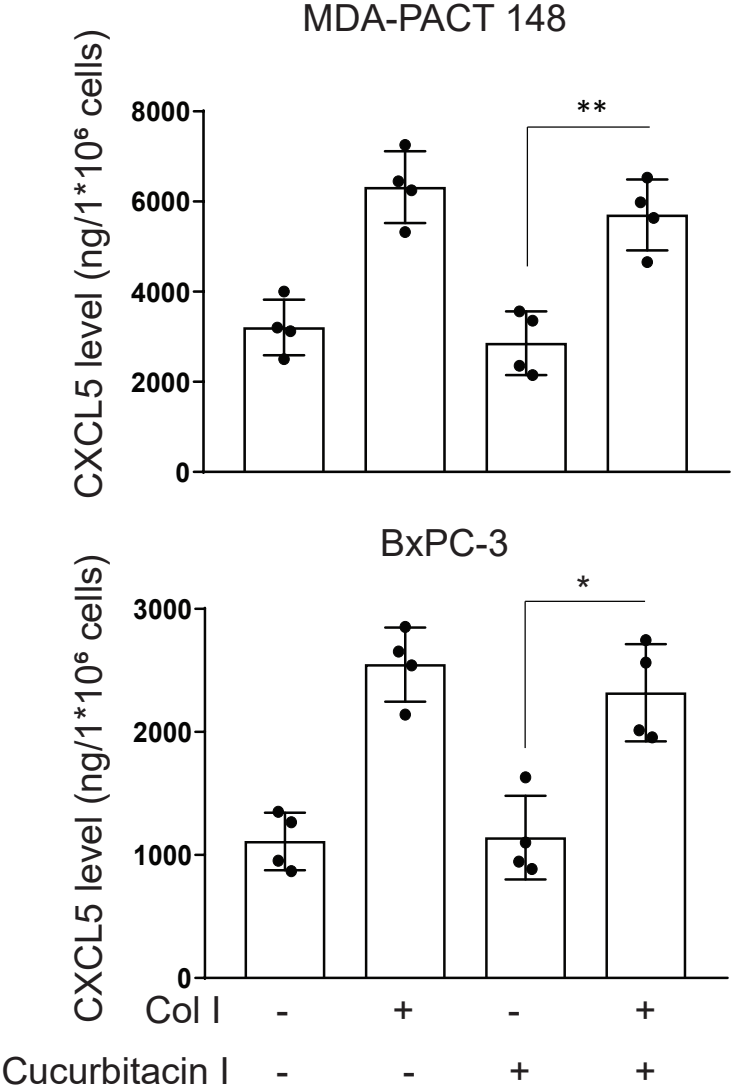


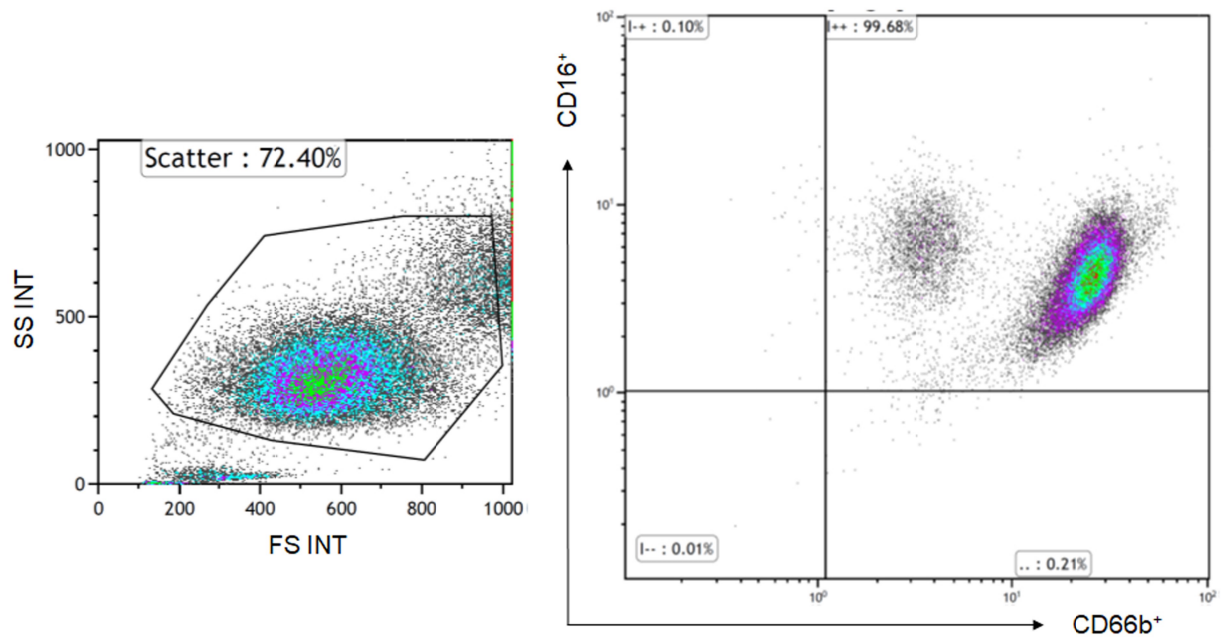
A.

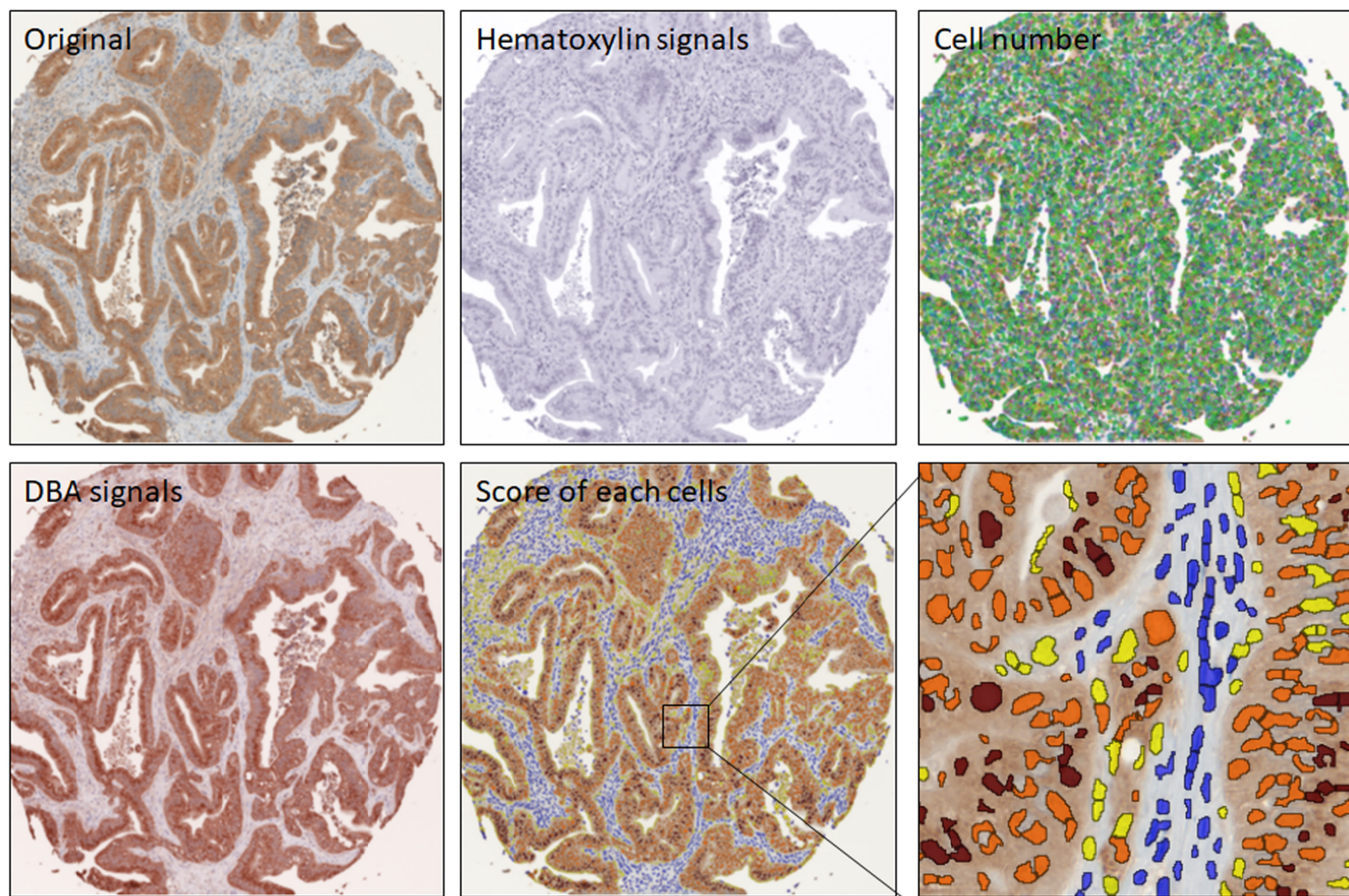


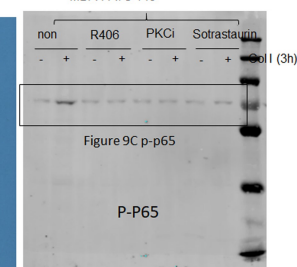
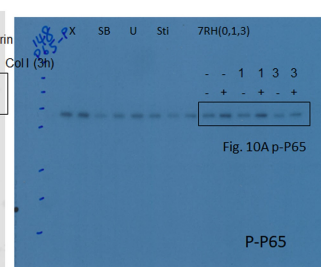
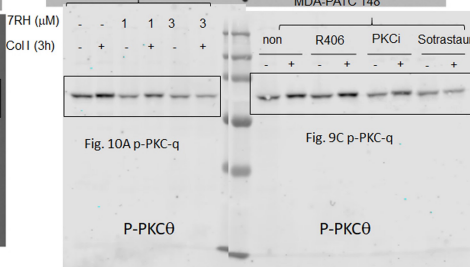
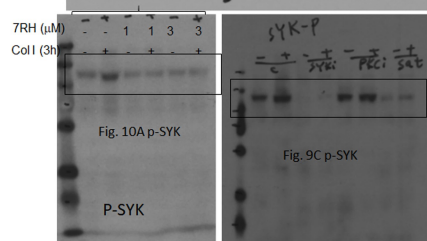
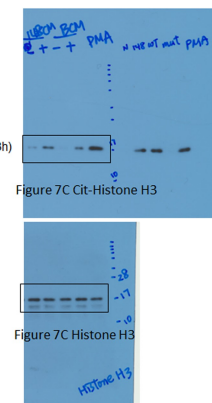
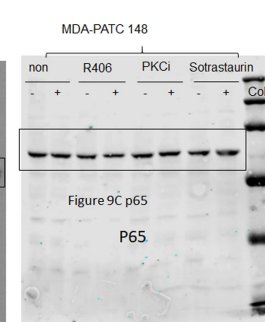
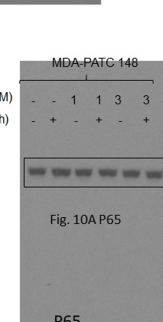
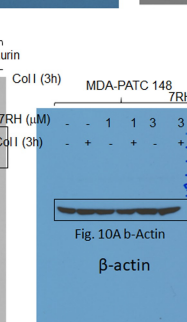
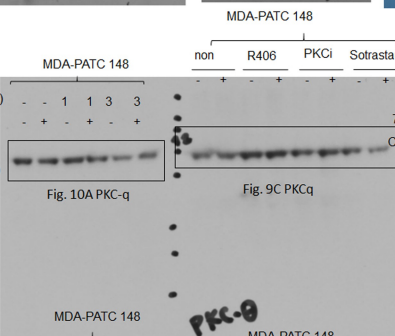
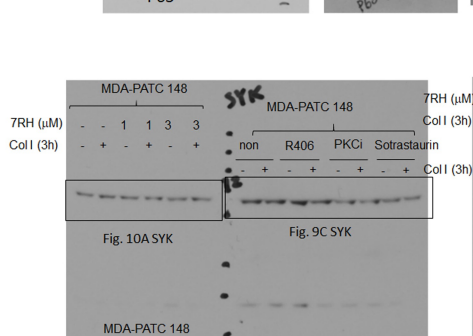
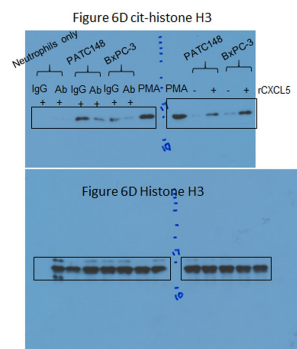
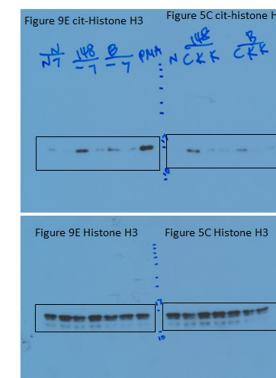
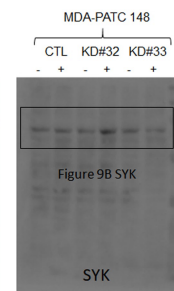
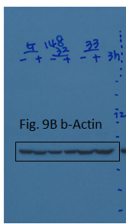
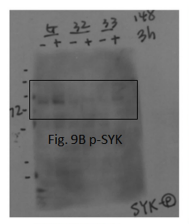
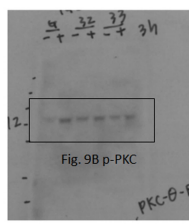
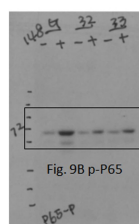
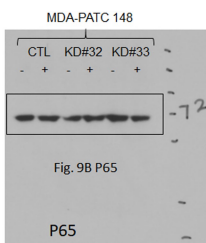
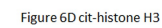
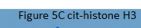
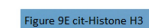
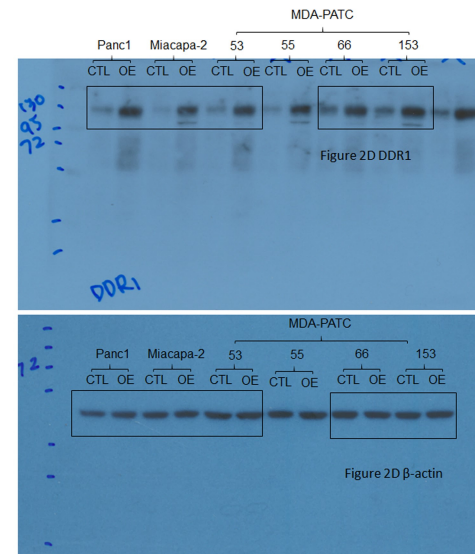
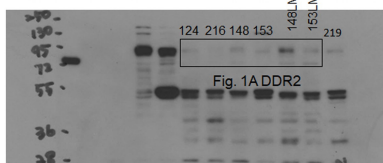
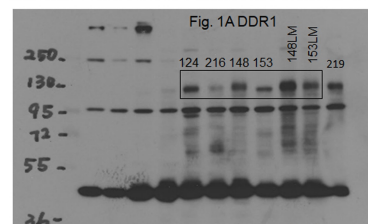
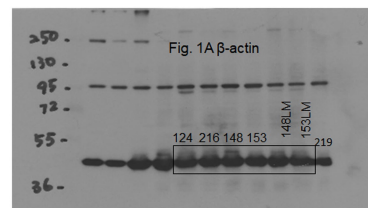
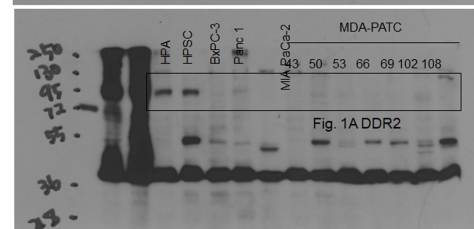
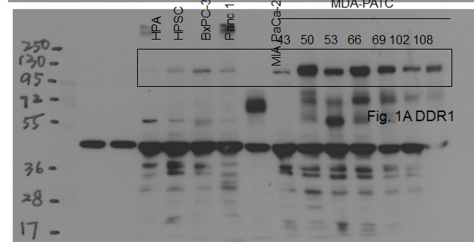
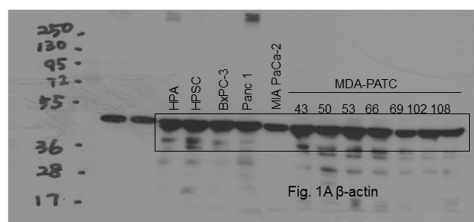
B.











Supplementary Table 1. The primers of real-time PCR and ChIP assay in the main text.

Primer for real-time PCR	Sequence 5' to 3'
hCXCL1-F	GAAAGCTTGCCTCAATCCTG
hCXCL1-R	CTTCCTCCTCCCTTCTGGTC
hCXCL2-F	GGGCAGAAAGCTTGTCTCAA
hCXCL2-R	GCTTCCTCCTTCCTTCTGGT
hCXCL3-F	CGCCCAAACCGAAGTCATAG
hCXCL3-R	GCTCCCCTTGTTCAGTATCTTTT
hCXCL5-F	TGGACGGTGGAAACAAGG
hCXCL5-R	CTTCCCTGGGTTCAAGAGAC
hCXCL6-F	AGAGCTGCGTTGCACTTGTT
hCXCL6-R	GCAGTTTACCAATCGTTTTGGGG
hCXCL7-F	GGCTTCCTCCACCAAAGGAC
hCXCL7-R	TCTTTGCCTTCGCCAAGTT
hCXCL8-F	GAATGGGTTTGCTAGAATGTGATA
hCXCL8-R	CAGACTAGGGTTGCCAGATTTAAC
hGAPDH-F	ACGGATTGGTCGTATTGGG
h-GAPDH-R	TGATTTTGGAGGGATCTCGC
Primer for ChIP assay	
CXCL5 promoter-NFkB-f-1	TAGAGGTGCACGCAGCTCCT
CXCL5 promoter-NFkB-r-1	GAGCACTGTGGCTTCCTCGT